FEBS Letters 365 (1995) 172–178 FEBS 15522

^1H and ^{13}C NMR assignment and secondary structure of *Chlorobium limicola* f. *thiosulfatophilum* ferrocytochrome c_{555}

Nathalie Morelle[a], Jean-Pierre Simorre[a], Michael Caffrey[a], Terrance Meyer[b], Michael Cusanovich[b], Dominique Marion[a,*]

[a]*Laboratoire de Résonance Magnétique Nucléaire, Institut de Biologie Structurale Jean-Pierre Ebel (CEA-CNRS), 41, avenue des Martyrs, 38027 Grenoble Cedex 1, France*
[b]*Department of Biochemistry, University of Arizona, Tucson, AZ 85721, USA*

Received 13 March 1995; revised version received 14 April 1995

Abstract **The ^1H resonances of the ferrocytochrome c_{555} from the anaerobic green sulfur bacterium *Chlorobium limicola* f *thiosulfatophilum* (strain Tassajara) have been assigned. Identification of spin systems and sequential assignment of ^1H was accomplished by automated assignment computer programs followed by manual verification. In addition, ^{13}C resonances have been extensively assigned by HSQC experiments at natural abundance. As determined by short-range NOE connectivities, $^{13}C^{\alpha}$ chemical shifts, and H^N exchange experiments, the secondary structure consists of 3 helices ranging from residues 3–13, 43–53 and 70–86. Interestingly, the second helix is significantly longer than observed by X-ray crystallography [1977, Proc. Natl. Acad. Sci. USA 74, 5244–5247]. A topological model of the cytochrome c_{555} is presented based on a small number of long-range NOE contacts. The helices are shown to pack onto the heme according to the pattern common to all class I cytochromes *c*.**

Key words: Protein NMR; Nuclear magnetic resonance spectroscopy; Automated assignment

1. Introduction

The class I cytochromes *c* are small soluble heme proteins that generally function as electron carriers between membrane-bound redox centers, such as the bc_1 complex and oxidases or photosynthetic reaction centers. Cytochromes *c* of this class are characterized by the CXXCH heme binding motif located near the amino terminus and a methionine located near the carboxy terminus which serves as the sixth heme ligand. The cytochrome c_{555} from the anaerobic green sulfur bacterium *Chlorobium limicola* f. *thiosulfatophilum* is a member of the class I cytochromes *c*, which presumably functions as a soluble carrier of electrons between the cytochrome bc_1 complex and the photosynthetic reaction center [1]. In addition, the *Chl. limicola* cytochrome c_{555} acts as a terminal electron acceptor in the oxidation of reduced sulfur compounds, presumably via a sulfite-cytochrome *c* oxidoreductase [1]. With respect to the mitochondrial cytochromes *c* and the prokaryotic cytochromes c_2, the best characterized members of the class I cytochromes *c*, the *Chl. limicola* cytochrome c_{555} exhibits two specific features: a smaller molecular weight (86 residues as compared to 103 for tuna cytochrome) and a lower redox potential (145 mV instead of 260 mV) [2]. Moreover, the *Chl. limicola* cytochrome c_{555} shares little sequence homology with other class I cytochromes *c* (24% with tuna cytochrome *c* and 24% with *Desulfovibrio vulgaris* cytochrome c_{553} [3]). Comparison of the low resolution crystal structure of *Chl. limicola* cytochrome c_{555} to that of mitochondrial cytochrome *c* reveals that the major difference in the polypeptide backbone, a 20 residue deletion between residues 33 and 34 in cytochrome c_{555}, is compensated by an inward folding of a subsequent loop over the heme [4]. Moreover, cytochrome c_{555} has been shown to exhibit significant structural similarities with *Azotobacter vinelandii* cytochrome c_5 and *Ectothiorhodospira halophila* cytochrome c_{551}, despite the low degree of sequence homology [5].

In our laboratory, we have been studying the structure and dynamic properties of cytochromes *c* from various species by NMR [5–7], in order to understand the underlying reasons for the differences observed in their electron transfer properties. In what follows, we present the assignment of the ^1H and ^{13}C resonances of *Chl. limicola* ferrocytochrome c_{555}. We will show that the secondary structure determined by NMR is somewhat different from that previously observed by X-ray crystallography. Finally, a topological model of the cytochrome c_{555} will be presented based on a small number of long-range NOE contacts.

2. Materials and methods

2.1. Sample preparation

Cytochrome c_{555} from *Chl. limicola* f. *thiosulfatophilum* (strain Tassajara) was purified as previously described [8]. For the NMR experiments in H_2O, the sample was concentrated at room temperature to approximately 8 mM in buffer containing 0.1 M K_2HPO_4/KH_2PO_4 (pH 6.0), 25 μM chloramphenicol (to inhibit bacterial growth), and 10 percent D_2O. Oxygen was removed by blowing argon gas over the solution surface for 15 min and the sample was reduced by addition of a 3-fold molar excess of sodium dithionite dissolved in 0.1 M K_2HPO_4/KH_2PO_4 buffer (pH 8.0). For the NMR experiments in D_2O, the sample was concentrated to approximately 4 mM in buffer containing 0.1 M K_2HPO_4/KH_2PO_4 (pH 6.0) and 100 percent D_2O. The D_2O sample was then deoxygenated and reduced in the same manner as the H_2O sample. Sample preparation in D_2O required approximately 30 min at room temperature.

*Corresponding author. Fax: (33) 76.88.54.94.

Abbreviations: NMR, nuclear magnetic resonance; NOE, nuclear Overhauser effect; PFG, pulsed B_0 field gradient; COSY-DQF, double quantum-filtered correlation spectroscopY; TOCSY, total correlation spectroscopy; NOESY, nuclear Overhauser and exchange spectroscopY; TPPI, time-proportional phase incrementation; HSQC, ^1H-detected heteronuclear single quantum coherence spectroscopy; J, scalar coupling constant.

This is publication No. 270 of the Institut de Biologie Structurale Jean-Pierre Ebel.

SSDI 0014-5793(95)00450-5

2.2. NMR experiments

All experiments were carried out on a Bruker AMX-600 spectrometer operating at ^1H = 600 MHz, equipped with a pulse-field gradient (PFG) unit. COSY-DQF [9], TOCSY [10] (with a 60 ms mixing time, plus further delays inserted to balance transverse and longitudinal cross-relaxation according to the 'clean TOCSY' technique) [11] and NOESY [12] (with a 150 ms mixing time) were recorded at 303 K, in phase sensitive mode with States-TPPI detection [13]. Aliphatic ^{13}C frequencies were obtained at natural abundance from a ^1H-^{13}C HSQC spectrum using PFG [14]. In addition, semi-selective TOCSY and NOESY experiments with the incremented dimension range restricted to the amide frequencies [15] were acquired at 298 and 308 K. Finally, a homonuclear 3D TOCSY-NOESY experiment was recorded at 303 K(TOCSY mixing time 60 ms plus delays, NOESY mixing time 150 ms) [16]. The amide proton exchange rates were evaluated from a set of semi-selective TOCSY experiments recorded in 30 min at several time points after exchanging the sample in D_2O [15]. Protons that were still observable after 24 h were considered in slow exchange.

The spectra were processed using either Bruker UXNMR or Felix version 2.3 (Biosym Technologies Inc.) software programs.

2.3. Computer-aided assignment

the assignment of the resonances was aided by the in-house computer program described in Fig. 1. Peaks are picked with Felix from the COSY, TOCSY and ^1H-^{13}C HSQC spectra and are sorted according to their chemical shift values [17–18] into regions corresponding to the specific correlations expected for the 17 different amino-acid types (no Arg, Gln or Phe residues are present in the cytochrome c_{555} sequence). This reduces the search space for a simulated annealing-based spin system detection routine (SA1), which matches the patterns of the expected amino-acid residues with the available peaks, while minimizing an energy corresponding to the number of peaks in the motif and their relative alignment.

In the second step, two matrices are built, reflecting respectively the possible amino-acid types for each of those spin system patterns, and all H^N-H^N, H^α-H^N and H^β-H^N NOESY peaks connecting each pair of patterns. A second simulated annealing algorithm (SA2) performs permutations in the sequence in order to bring together the peaks connected by NOEs while satisfying the amino-acid types along the sequence. The user can modify or augment the patterns identified by SA1, and assign some specifically to accomodate manual assignments. The spin-system detection and the SA2 protocols have since then been implemented in Felix (Felix_Assign July 1994 release).

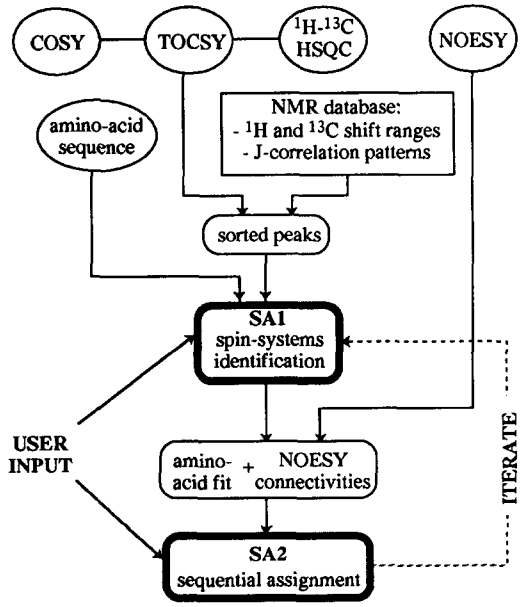

Fig. 1. Flow-chart diagram of the computer assignment program.

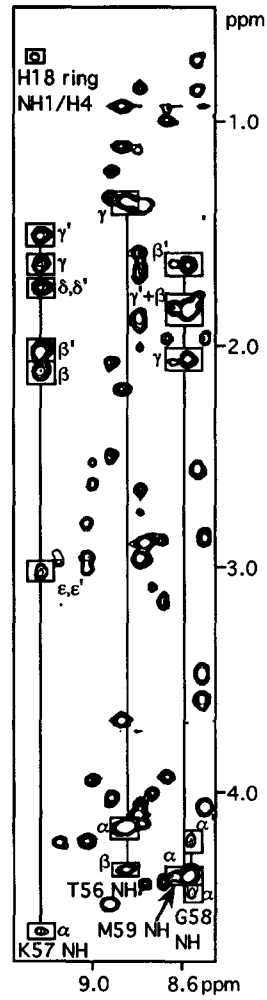

Fig. 2. Part of the H^N-aliphatic region of the ^1H-^1H TOCSY spectrum of *Chl. limicola* ferrocytochrome c_{555}. The assignment of the peculiarly broad resonances of residues 56–59 is shown.

3. Results and discussion

3.1. General aspect of the data

The NMR spectra of cytochrome c_{555} suggest at first sight that the molecule consists largely of α-helices: this is shown by the small number of H^N and H^α resonances in the downfield part of their allowed range and by the rather small $^3J_{H^N H^\alpha}$ coupling constants evident form the COSY cross-peak footprint. In comparison to other cytochromes *c* [5–6,19], the resonances of cytochrome c_{555} exhibit broader line widths (see Fig. 2): for example, the linewidth at half-height of the well-resolved meso-5 and meso-20 signals, as evaluated on a 1D spectrum, are 16 ± 2 Hz and 24 ± 2Hz, respectively. For *E. halophila* ferrocytochrome c_{551}, which possesses slightly fewer amino-acid residues (78 residues), both line widths are 10 ± 2 Hz. Broad lines may be due either to efficient dipole-dipole relaxation or chemical exchange at an intermediate rate. Short transverse relaxation originates from slow molecular motions, i.e. slow tumbling rates of the molecule. Proteins of similar size dissolved in the same solvent (H_2O) usually show narrower signals, thus aggregation can be postulated. Light scattering experi-

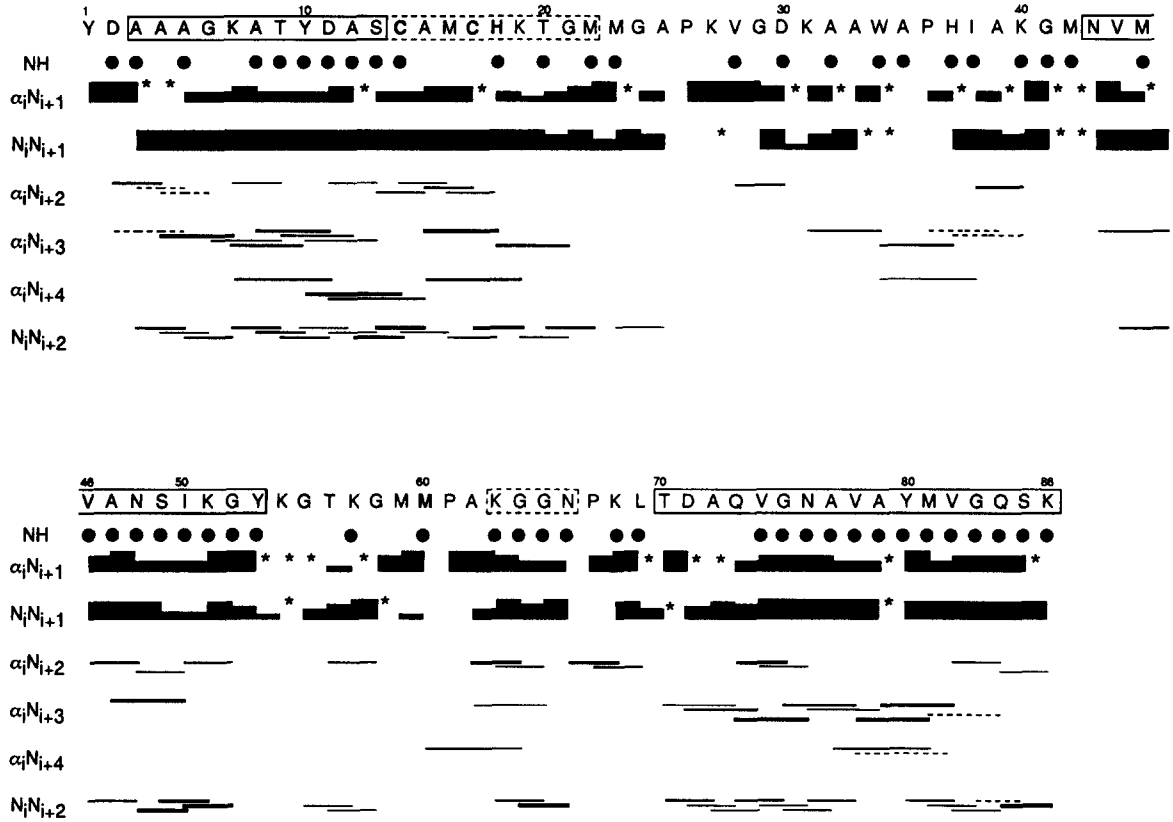

Fig. 3. Schematic summary of the sequential connectivities for the ^1H assignment of *Chl. limicola* ferrocytochrome c_{555}. The intensity of the NOEs is reflected by either bar height or line thickness. Dotted lines correspond to NOEs for which overlap of peaks hindered an accurate quantification. Asterisks indicate sequential connectivities which could not be seen due to spectral overlap. In addition, H^N protons that were still observable 24 h after exchange in D_2O are indicated by filled circles. The residues belonging to helical fragments are shown in boxes.

ments suggest a certain amount of high molecular weight aggregates in the solution, but no major oligomer is present. The line broadening is thus probably due to chemical or conformational exchange. The purity of the sample has been checked by gel electrophoresis and UV spectrometry, and no degraded portion of the protein appears to be responsible for this phenomenon. Residues 55–60 (M60 being the 6th heme ligand) and the heme meso-15 proton show particularly broad H^N line widths. In the case of M59 H^N and the meso-15 proton, a splitting of the frequency is present. This has been observed previously on other cytochromes (Pierre Gans, personal communication) and might be due either to conformational exchange around the ligand methionine or to a covalently modified methionine (e.g. methionine sulfone and/or sulfoxide). The second hypothesis has been confirmed by mass analyses of the oxidised protein, which exhibits two peaks at M + 16 (methionine sulfone) and M + 32 (methionine sulfoxide) in addition to the expected peak at M = 9,395 Da (data not shown). Reduction with dithionite does not restore the reduced amino-acid.

3.2. Spin system identification

The automated spin-system detection was used (SA1, Fig. 1). Due to the linewidth in the data and the presence of numerous long-chain residues (11 lysines and 8 methionines, for which the isotropic transfer was not always efficient enough to correlate the H^N with all side-chain protons), significant overlap occurred and many peaks were missing, which limited the performance of the automated routines. Nonetheless, approximately 50% of the spin systems were detected automatically; the remaining peaks were assigned manually. The HSQC spectrum was used both automatically and manually to check the side-chain assignment and the amino-acid identification from the ^{13}C chemical shift ranges. In addition, the HSQC spectrum allows a straightforward recognition of methylene proton pairs.

The assignment of the resonances of the heme was performed manually using the NOESY spectrum. The results are consistent with those previously obtained by Senn et al for the reduced state [20]. The signals for the ^1H of the heme propionates are very weak; consequently these resonances could only be partially and non-specifically assigned.

3.3. Sequential assignment

One of the cysteines connected to the heme (C14) and the sixth iron ligand (M60) were identified unambiguously by their unusually low chemical shifts. They provided anchor points for the second part of the program (SA2, Fig. 1), which unambiguously assigned residues 9–15, 52–60 and 67–70 (the assignments for the other parts of the sequence were not reproducible). This substantially facilitated the task of assigning the remaining residues. The spectra at 298 and 308 K, although showing few chemical shift differences, and the 3D TOCSY-NOESY spectrum removed some ambiguities, especially in the region spanning residues 40–50, where the overlap between residues 47 and 49 hindered the assignment. The assignments

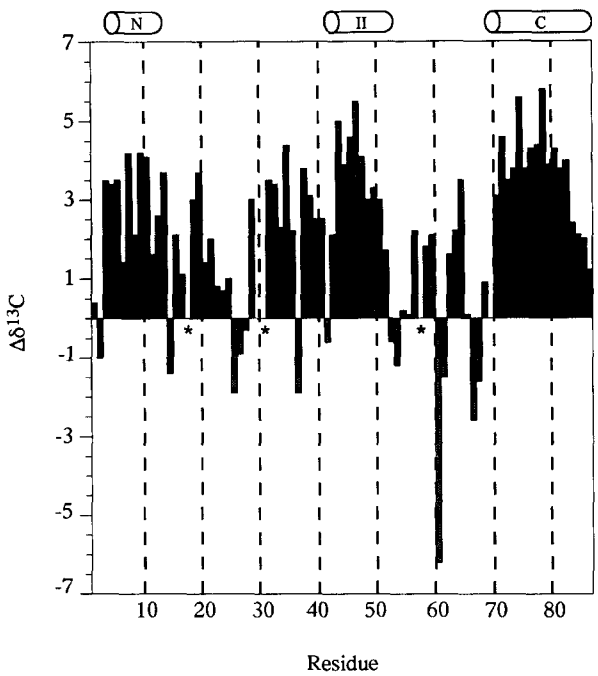

Fig. 4. Secondary $^{13}C^{\alpha}$ chemical shifts of *Chl. limicola* ferrocytochrome c_{555}. The secondary shifts have been computed as $\Delta\delta = \delta obs - \delta rc + 2.81$, where δrc are the random coil values given in [21] and the 2.81 ppm accounts for a difference in the ^{13}C calibration. Asterisks indicate unassigned resonances. The helical fragments suggested by the NMR data are shown by cylinders above the graph.

are given in Table 1 and a summary of the short and medium range NOEs is displayed in Fig. 3.

3.4. Secondary structure

The secondary structure patterns were determined using the classical approach based on short- and medium range NOE and H^N exchange rates. They were confirmed using the secondary $^{13}C^{\alpha}$ chemical shifts shown in Fig. 4, which have proven to be characteristic of the secondary structure [21]. In diamagnetic heme proteins, the ring current of the porphyrin also contributes to the chemical shift: whereas the ^1H chemical shift can be significantly biased by this effect (due to the small frequency range for this nucleus (10 ppm)), ^{13}C NMR results obtained for other cytochromes [5,7,14] have shown that the ring current shift has a minor impact on ^{13}C chemical shift.

The 2.8 Å X-ray crystal structure of cytochrome c_{555} possesses an N-terminal helix from residue 1 to 11, type I hairpin loops from residues 20 to 40, a short helix from residue 42 to 46, no regular structure from 47 to 59, and a C-terminal helix from residue 72 to 86. There is some level of uncertainty in the crystal structure for the configuration of regions ranging from residues 32 to 36 and 65 to 70 [4]. As can be seen in Figs. 3 and 4, the NMR data identify the N-terminal helix from residues 3 to 13. A second helix extends from residues 43 to 53, which is approximately two turns longer than the fragment detected in the crystal structure. Finally the C-terminal helix is located from residues 70 to 86. No other well-defined secondary structure element has been observed by NMR. Nevertheless, the NOE data alone (Fig. 3) suggest distorted helices in segments 14–22 (just after the N-terminal helix and through the heme binding site), as previously observed in other cytochromes *c* [6], and 63–66 (between the sixth heme ligand and the C-terminal helix).

3.5. Topological model

From the NMR assignment, typical features of cytochromes *c* can be recognised, which give some preliminary insight into the three-dimensional structure of *Chl. limicola* ferrocytochrome c_{555}. A topological model of cytochrome c_{555} is presented in Fig. 5. As stated above, three of the helices typical of the cytochromes *c* are present in cytochrome c_{555}. From a few long range NOE restraints we can recognise the characteristic folding of such cytochromes [22]. Several NOEs suggest a contact between the N- and C-terminal helices, for instance between D2 and N76, Y10 and A77. Furthermore, the line widths of the aromatic resonances of Y10 and Y80 are broad, indicating that the flipping rate of the rings is of intermediate range (with respect to the chemical shift difference) , as compared to the other tyrosines Y1 and Y53 which are in fast rotation. The interaction of the N- and C-terminal helices is a widely conserved feature in cytochromes *c*, and aromatic residues are always present in these two structural elements. Their hydrophobic interaction likely stabilises the overall fold of the protein and their mutual steric hindrance results in most cases in line broadening (e.g. Y6 and Y73 of *E. halophila* cytochrome c_{551} [5], Y7 and Y75 of *D. vulgaris* cytochrome c_{553} [6]).

In the region adjacent to the heme binding site, the sidechains of A25 and P26 exhibit resonances shifted several ppm upfield from random coil values by the ring current effect of the heme (A25 βCH_3 at −1.54 ppm, P26 β and γ protons under 1 ppm, see Table 1). Their proximity to the heme group is confirmed by several NOEs to H18, the histidine ligand. These residues are well-conserved among most cytochrome *c* sequences. Very similar shifts have been observed for *E. halophila* ferrocytochrome c_{551} [5] with A25 βCH_3 at −1.30 ppm and P26 protons shifted upfield, and for the A22 βCH_3 of *D. vulgaris* ferrocytochrome c_{553} (−0.88 ppm) [6].

The NOE pattern in the next segment, residues 27–42, shows an absence of regular secondary structure, and contacts between residues P26 and H37, V28 and W34 suggest the presence

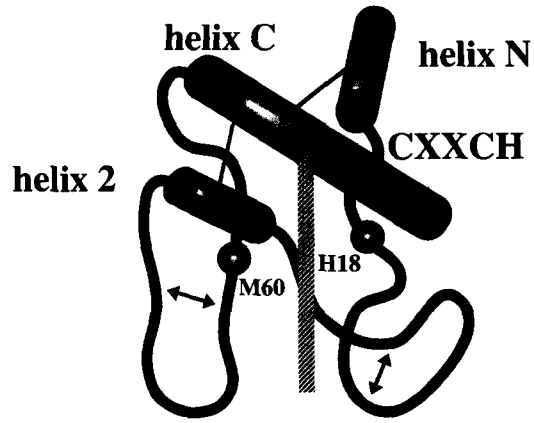

Fig. 5. Topological model of *Chl. limicola* ferrocytochrome c_{555} tertiary structure based on a small number of long-range NOEs (see text). Axial ligands are denoted by spheres. Helices are presented as cylinders. The medium and long range NOEs which allowed us to design the model are marked by arrows. This schematic drawing locates the different structural elements along the sequence, but is not meant to represent the exact tertiary structure of the protein.

Table 1
^{1}H and ^{13}C-NMR resonance assignment of *Chl. limicola* ferrocytochrome c_{555} at 30°C and pH 6.0

Protein resonances

Residue	^{1}H (^{13}C) chemical shifts (ppm)			
	NH	CαH	CβH	others
Tyr[1]	–	4.21 (56.2)	3.27 2.74 (37.2)	H2, H6 7.22; H3, H5 6.91
Asp[2]	8.39	4.86 (50.3)	2.79, 2.49 (39.9)	
Ala[3]	8.81	4.15 (53.2)		$C\beta H_3$ 1.39 (16.7)
Ala[4]	8.07	4.18 (53.1)		$C\beta H_3$ 1.51 (15.6)
Ala[5]	7.70	4.19 (53.2)		$C\beta H_3$ 1.45 (16.8)
Gly[6]	8.23	3.97, 3.76 (43.6)		
Lys[7]	7.20	2.70 (58.1)	1.56 (30.5)	CγH 1.20, 0.71 (22.8); CεH 3.15
Ala[8]	7.76	4.19 (51.8)		$C\beta H_3$ 1.49 (16.0)
Thr[9]	7.38	4.17 (64.5)	4.28 (67.4)	$C\gamma H_3$ 1.50 (21.0)
Tyr[10]	8.76	4.01 (59.9)	3.09, 2.88 (36.2)	H2, H6 7.72; H3, H5 7.05
Asp[11]	9.03	3.95 (52.9)	2.62, 2.54 (38.1	
Ala[12]	7.47	4.43 (52.3)		$C\beta H_3$ 1.64 (18.1)
Ser[13]	8.59	5.27 (59.2)	4.59, 4.36 (65.0)	
Cys[14]	8.19	6.15 (53.8)	2.79, 2.69 (34.5)	
Ala[15]	8.03	3.21 (51.8)		$C\beta H_3$ 0.96 (16.2)
Met[16]	8.36	4.10 (54.9)	2.28 (29.5)	$C\gamma H_3$ 2.88, 2.80 (29.7)
Cys[17]	6.41	4.70	2.56, 1.35 (34.7)	
His[18]	6.60	2.51 (56.0)	2.03, 1.32 (26.5)	N1H 9.28; H2 0.74; H4 0.70
Lys[19]	8.83	4.11 (57.6)	1.89 (30.5)	
Thr[20]	7.54	4.27 (61.7)	4.32 (68.0)	$C\gamma H_3$ 1.05 (19.3)
Gly[21]	7.07	3.72, 3.65 (44.2)		
Met[22]	7.68	4.30 (54.6)	2.17, 2.00 (31.2)	CγH 2.72, 2.64 (30.0)
Met[23]	9.05	4.22 (54.5)	2.96, 2.83 (27.9)	CγH 3.02, 2.81 (31.6)
Gly[24]	7.98	4.32, 3.50 (43.2)		
Ala[25]	7.26	3.13 (47.8)		$C\beta H_3$ – 1.53 (13.9)
Pro[26]	–	3.63 (59.2)	0.81, – 0.54 (26.0)	CγH – 0.26, – 0.36 (23.9); CδH 2.99, 1.64 (46.8)
Lys[27]	8.10	3.93 (53.6)	1.98, 1.17 (31.0)	CγH 1.02 (21.9); CδH 1.47 (26.8); CεH 2.87
Val[28]	8.12	3.14 (63.2)	1.56 (30.5)	$C\gamma H_3$ 0.29 (22.9), 0.18 (18.8)
Gly[29]	8.23	4.19, 3.68 (42.2)		
Asp[30]	7.99	4.72	3.48, 2.14 (39.2)	
Lys[31]	8.28	4.15 (57.4)	1.75 (30.5)	CγH 1.46, 1.13 (26.6); CδH 1.58 (26.9)
Ala[32]	8.19	4.24 (53.1)		$C\beta H_3$ 1.48 (16.0)
Ala[33]	7.95	4.39 (52.0)		$C\beta H_3$ 1.65 (13.2)
Trp[34]	7.91	4.08 (59.4)	3.36, 3.08 (27.7)	NH 7.10; H2 7.32; H4 7.56; H5 7.32; H6 5.92; H7 5.48
Ala[35]	7.95	4.06 (51.9)		$C\beta H_3$ 1.30 (16.7)
Pro[36]	–	4.49 (58.2)	2.27, 1.64 (28.8)	CγH 2.04, 1.84 (25.9); CδH 3.89, 3.74 (48.2)
His[37]	7.30	4.42 (56.8)	3.81 (26.5)	H2 9.43; H4 7.73
Ile[38]	8.69	3.95 (62.9)	1.98 (36.5)	CγH 1.18 (28.5); $C\gamma H_3$ 1.00 (15.0); $C\delta H_3$ 0.96 (12.6)
Ala[39]	7.95	4.19 (52.2)		$C\beta H_3$ 1.49 (16.0)
Lys[40]	7.81	4.19 (56.4)	2.17	CγH 1.97 (23.2); CδH 1.46 (27.6), 1.44; CεH 3.05
Gly[41]	7.68	4.68, 3.93 (41.6)		
Met[42]	7.70	4.33 (55.9)		
Asn[43]	8.80	4.40 (54.8)	4.70, 2.89 (34.9)	NH 7.22, 6.91
Val[44]	7.60	3.70 (64.1)	1.91 (29.6)	$C\gamma H_3$ 1.05 (20.7), 0.93 (19.9)
Met[45]	7.99	4.61 (58.4)	2.72, 2.48 (34.2)	CγH 2.94, 2.70 (31.3)
Val[46]	8.90	3.68 (65.7)	2.21 (29.5)	$C\gamma H_3$ 1.12 (21.8), 0.94 (19.4)
Ala[47]	7.72	3.99 (53.8)		$C\beta H_3$ 1.44 (15.8)
Asn[48]	8.53	4.07 (52.8)	2.86, 1.98 (34.6)	NH 8.31, 6.11
Ser[49]	7.74	2.54 (58.8)	3.49, 3.13 (60.6)	
Ile[50]	7.65	3.31 (62.8)	1.66 (36.6)	CγH 0.65 (28.4); $C\gamma H_3$ 0.72 (15.1); CδH 0.79 (12.1)
Lys[51]	7.74	3.90 (55.6)	1.72 (31.2)	
Gly[52]	7.12	3.57, 2.75 (41.6)		
Tyr[53]	7.85	4.30 (54.6)	2.47, 2.40 (38.1)	H2, H6 6.35; H3, H5 6.54
Lys[54]	8.01	4.25 (54.1)	1.67	CγH 1.23 (22.6), 1.16; CδH 1.53, 1.42; CεH 2.89
Gly[55]	7.88	4.65, 4.07 (42.3)		
Thr[56]	8.89	4.16 (62.5)	4.36 (67.2)	$C\gamma H_3$ 1.37 (20.2)
Lys[57]	9.28	4.63	2.14, 2.04 (31.9)	CγH 1.65, 1.52 (22.9); CδH 1.74 (26.4); CεH 3.04
Gly[58]	8.60	4.44, 4.21 (44.0)		
Met[59]	8.62	4.37 (55.9)	1.85, 1.64 (31.9)	CγH 2.07, 1.85 (29.6)
Met[60]	7.59	1.45 (47.6)	– 0.20, – 2.20 (25.0)	CγH – 1.78, – 2.79 (26.9); $C\delta H_3$ – 2.99 (14.7)
Pro[61]	–	3.45 (58.6)	1.68, 0.90 (29.6)	CγH 1.47, 0.75 (24.0); CδH 2.90, 0.96 (47.5)
Ala[62]	7.75	2.84 (51.3)		$C\beta H_3$ 0.87 (15.5)
Lys[63]	8.82	2.97 (56.1)	1.71 (32.1)	CδH 1.60, 0.87 (25.6)
Gly[64]	7.11	4.32, 2.57 (45.7)		
Gly[65]	7.92	4.26, 3.52 (42.3)		
Asn[66]	7.33	5.37 (47.2)	3.43, 2.89 (36.4)	NH 7.38, 7.25

Table 1 (*continued*)

Protein resonances

Residue	^{1}H (^{13}C) chemical shifts (ppm)			
	NH	CαH	CβH	others
Pro^{67}	-	4.25 (58.5)	2.23, 1.97 (31.0)	Cγ**H** 1.97, 1.88 (23.6); Cδ**H** 3.92, 3.70 (48.7)
Lys^{68}	7.63	4.15 (54.8)	1.94, 1.88	Cγ**H** 1.52, 1.42 (23.3); Cδ**H** 1.71; Cε**H** 3.01, 2.88
Leu^{69}	7.25	4.50 (52.9)	1.83, 1.45 (41.0)	Cγ**H** 1.91 (28.6); Cδ**H**$_3$ 1.16 (24.6), 0.94 (21.5)
Thr^{70}	8.96	4.50 (63.4)	4.77	Cγ**H**$_3$ 1.36 (19.6)
Asp^{71}	8.82	4.06 (55.9)	2.66 (37.2)	
Ala^{72}	8.31	4.21 (53.2)		Cγ**H**$_3$ 1.48 (16.0)
Gln^{73}	7.87	4.21 (57.2)	2.55, 2.13 (26.9)	Cγ**H** 2.55 (33.1); NH 7.53, 6.75
Val^{74}	8.10	3.75 (65.8)	2.16 (29.2)	Cγ**H**$_3$ 0.95 (22.1, 20.8)
Gly^{75}	8.54	3.60, 3.49 (46.0)		
Asn^{76}	8.71	4.40 (54.1)	3.15, 2.88 (34.8)	NH 7.81, 7.34
Ala^{77}	8.36	4.29 (54.1)		Cβ**H**$_3$ 2.12 (16.8)
Val^{78}	8.94	4.04 (66.0)	2.50 (29.6)	Cγ**H**$_3$ 2.10 (23.3), 1.23 (21.0)
Ala^{79}	8.34	3.77 (53.6)		Cβ**H**$_3$ 1.40 (14.9)
Tyr^{80}	8.35	3.92 (60.1)	3.58, 2.96 (34.9)	H2, H6 6.54; H3, H5 6.18
Met^{81}	8.09	2.48 (57.6)	2.43, 1.68 (30.5)	Cγ**H** 1.27; Cδ**H**$_3$ −0.46 (13.0)
Val^{82}	8.56	2.56 (64.2)	1.81 (29.6)	Cγ**H**$_3$ 0.87 (22.3), 0.74 (18.6)
Gly^{63}	7.64	3.68, 3.57 (44.6)		
Gln^{84}	6.51	3.96 (55.5)	1.76, 1.10 (28.3)	Cγ**H** 1.44, 1.26 (30.6); NH 6.93, 6.47
Ser^{85}	7.12	4.10 (57.5)	3.55, 2.62 (62.2)	
Lys^{86}	6.98	4.10 (55.1)	1.71, 1.64 (31.9)	Cγ**H** 1.41, 1.27 (21.7); Cδ**H** 1.53 (27.4); Cε**H** 2.86

Heme resonances

Meso H		Ring methyl		Thiomethine		Thiomethyl		Propionate[a]	
5	10.05	2^1	3.77 (15.2)	3^1	5.98 (34.5)	3^2	1.92 (20.4)	a^1	4.48, 3.59 (22.8)
10	9.50	7^1	3.96 (13.2)	8^1	6.18 (37.5)	8^2	2.29 (21.5)	a^2	
15	9.76	12^1	3.04 (11.4)					b^1	4.14, 3.81 (24.5)
20	9.74	18^1	3.72 (14.4)					b^2	2.76 (40.0)

IUPAC nomenclature. ^{1}H chemical shifts are given ± 0.02 ppm, and were referenced with respect to the water resonance at 4.725 ppm. ^{13}C chemical shifts (indicated in parentheses after the corresponding protons) are given ± 0.15 ppm, and were referenced to TMS.
[a] Two different spinsystems, a and b, have been partially indentified for the propionates, but could not be specifically assigned to propionates 13 and 17.

of a loop. The crystal structure consists of several hairpin loops while most cytochromes *c* contain an Ω-loop in this region.

The second conserved helix is surprisingly short in the crystal structure, consisting of a single turn. The NMR data (in particular the exchange rates which are very slow for residues 45–53) suggest a helix of approximately 10 residues (43 to 53). Moreover this segment shows several NOE contacts with the C-terminal helix. This is in agreement with the characteristic fold of cytochromes *c*. The next segment extends from residue 54 to the sixth heme ligand M60. In the crystal structure it forms a long loop, which is consistent with several medium-range NOEs observed by NMR. The C-terminal helix itself folds behind the heme, which is suggested by the peculiar shift of M81 S-methyl (−0.46) and NOEs with the heme protons.

Interestingly, cytochrome c_{555} shares a singularity with *E. halophila* cytochrome c_{551}: the most upfield shifted heme ring methyl carbon is 12^1, unlike other cytochromes where 18^1 has the lowest chemical shift. This might indicate a different geometry of the heme ligands as previously discussed [5].

The calculation of a high resolution structure using the NMR constraints is now in progress in our laboratory. We anticipate that an improved *Chl. limicola* ferrocytochrome c_{555} structure will allow for a better characterisation of the interaction with reaction partner proteins such as flavocytochrome *c* [23], and facilitate understanding of its unusual redox properties.

Acknowledgements: We wish to thank Dr. F. Guerlesquin and C. Sebban (University of Marseille) for help in sample preparation, Dr. O. Dideberg and G. Sainz (IBS) for help in the light-scattering experiments, and Dr. E. Forest and C. Saint Pierre-Monnet (IBS) for the mass analysis. This work was supported in part by the Commissariat à l'Energie Atomique (CEA), the Centre National de la Recherche Scientifique (CNRS), Biosym Technologies Inc., and the United States Public Health Services (Grant GM 21277 to M. Cusanovich). N. Morelle is the recipient of a Biosym Technologies-CEA fellowship. M. Caffrey gratefully acknowledges support of the Human Frontiers of Science Program and the CNRS.

References

[1] Kusai, K. and Yamanaka, T. (1973) Biochim. Biophys. Acta 325, 304–314.
[2] Pettigrew, G.R. and Moore, G.W. (1987) In: Cytochromes *c*: Biological Aspects, Springer-Verlag, Berlin.
[3] Moore, G.W. and Pettigrew, G.R. (1990) In: Cytochromes *c*: Evolutionary, Structural and Physiological Aspects, Springer-Verlag, Berlin.
[4] Korszun, Z. and Salemme, F. (1977) Proc. Natl. Acad. Sci. USA 74, 5244–5247.
[5] Bersch, B., Brutscher, B., Meyer, T.E. and Marion, D. (1995) Eur. J. Biochem. 227, 249–260.
[6] Marion, D. and Guerlesquin, F. (1992) Biochemistry 31, 8171–8179; Blackledge, M.J., Medvedeva, S., Poncin, M., Guerlesquin, F., Bruschi, M. and Marion, D. (1995) J. Mol. Biol. 245, 661–681

[7] Caffrey, M., Brutscher, B., Simorre, J.-P., Fitch, J., Cusanovich, M. and Marion, D. (1994) Eur. J. Biochem. 221, 63–75.
[8] Meyer, T.E. (1994) Methods Enzymol. 243, 426–435.
[9] Rance, M., Sørensen, O.W., Bodenhausen, G., Wagner, G. Ernst, R.R. and Wüthrich, K. (1983) Biochem. Biophys. Res. Commun. 117, 479–485.
[10] Braunschweiler, L. and Ernst, R.R. (1983) J. Magn. Reson. 53, 521–528; Davis, D.G. and Bax, A. (1985) J. Am. Chem. Soc. 107, 2820–2821.
[11] Griesinger, C., Otting, G., Wüthrich, K. and Ernst, R.R. (1988) J. Am. Chem. Soc. 110, 7870–7872.
[12] Macura, S., Huang, Y., Suter, D. and Ernst, R.R. (1981) J. Magn. Reson. 43, 259–281.
[13] Marion, D., Ikura, M., Tschudin, R. and Bax, A. (1989) J. Magn. Reson. 85, 393–399.
[14] Medvedeva, S., Simorre, J.-P., Brutscher, B., Guerlesquin, F. and Marion, D. (1993) FEBS Lett. 333, 251–256; Bax, A. and Pochapsky S. (1992) J. Magn. Reson. 99, 638–643.
[15] Brutscher, B., Simorre, J.-P. and Marion, D. (1992) J. Magn. Reson. 100, 416–424.
[16] Oschkinat, H., Cieslar, C and Griesinger, C. (1990) J. Magn. Reson. 86, 453–469; Vuister, G.W., Boelens, R., Padilla, A., Kleywegt, G.J. and Kaptein, R. (1990) Biochemistry 29, 1829–1839; Simorre, J.-P. and Marion, D. (1991) J. Magn. Reson. 94, 426–432.
[17] Groβ, K.-H. and Kalbitzer, H.R. (1988) J. Magn. Reson. 76, 87–89.
[18] Richarz, R. and Wüthrich, K. (1978) Biopolymers 17, 2133–2141 and Wishart, D.S., Sykes, B.D. and Richards, F.M. (1991) J. Mol. Biol. 222, 311–333.
[19] Wand, A.J., Di Stefano, D.L., Feng, Y., Roder, H. and Englander, S.W. (1989) Biochemistry 28, 186–194; Williams, G., Moore, G.R., Porteous, R., Robinson, M.N., Soffe, N. and Williams, R.J.P. (1985) J. Mol. Biol. 183, 409–428.
[20] Senn, H., Cusanovich, M. and Wüthrich, K. (1984) Biochim. Biophys. Acta 785, 46–53.
[21] Wishart, D.S. and Sykes, B.D. (1994), J. Biomol. NMR 4, 171–180.
[22] Chotia, C. and Lesk, A.M. (1985) J. Mol. Biol. 182, 151–158.
[23] Davidson, M.W., Meyer, T.E., Cusanovich, M.A. and Knaff, D.B. (1986) Biochim. Biophys. Acta 850, 396–401.